SCIENCE CHINA
Information Sciences

• **Supplementary File** •

A compact polarization-integrated long wavelength infrared focal plane array based on InAs/GaSb superlattice

Jian ZHOU[1], Yi ZHOU[1,2*], Ying SHI[1], Fangfang WANG[1], Zhicheng XU[1], Zhizhong BAI[1], Min HUANG[1], Lulu ZHENG[1], Zhaoming LIANG[1], Yihong ZHU[1], Qingqing XU[1], Yiming SHEN[1], Xiangxiao YING[1] & Jianxin CHEN[1,2*]

[1]*Key Laboratory of Infrared Imaging Materials and Devices, Shanghai Institute of Technical Physics, Chinese Academy of Sciences, Shanghai* 200083*, China;*
[2]*Hangzhou Institute for Advanced Study, University of Chinese Academy of Sciences, No.1, Sub-Lane Xiangshan, Xihu District , Hangzhou* 310024*, China*

Appendix A Simulation and calculation method

The detailed optical behavior of the PI-FPA for each considered wavelength can be solved by applying electromagnetic (EM) theory. The incident plane wave propagates along the negative z-direction and polarizes with the electric field parallel to the x(TE) and y(TM) direction, respectively. The incident electric field intensity is assumed to be Ex= Ey = [1V/m] exp(-jkz). In general application, it is necessary to know the photocurrent generated by the incident light of a specific wavelength per unit intensity, so the responsivity is introduced to characterize the relationship between the incident light power and the generated photocurrent, expressed as [1, 2]

$$R_v = \frac{q\lambda}{hc} QE \tag{A1}$$

where q is electric charge, h is plank constant, λ is incident light, and c is light speed in vacuum, and the quantum efficiency (QE) equals absorption efficiency without considering recombination, if every absorbed photon is transformed as a photon-generated carrier. The absorption A(λ) per unit volume is defined as [3–5] and the transmission per unit area among z direction is expressed as [5]

$$A(\lambda) = \frac{1}{a^2} \int_v \varepsilon'' |E(\lambda)|^2 dxdydzd\lambda \tag{A2}$$

$$T(\lambda) = \frac{1}{a^2} \int_s P_z dxdyd\lambda \tag{A3}$$

where $|E(\lambda)|^2$ the normalized total intensity, P_z the normalized energy flow, ε'' the imaginary part of dielectric function of T2SL, and dλ the wavelength step used in this simulation. a is the pixel center distance, respectively. The reflectivity (R) and transmittance (T) of the bare Si substrate are satisfied as follows [6]

$$R = (\frac{n-1}{n+1})^2 \tag{A4}$$

$$T = \frac{(1-R)^2 e^{-\alpha t}}{1 - R^2 e^{-2\alpha t}} \tag{A5}$$

where α, n, and t is the absorption coefficient, refractive index and thickness of Si substrate, which is 0, 3.42 in the wavelengths (3-15 um) and 200 um in our work, respectively. As results, the transmittance of bare Si substrate is about 56%.

Appendix B Optimized parameters of grating

The schematic diagram of the subwavelength metal grating was shown in Figiure B1(a). The ER spectra as function of different periods, linewidths, and heights was shown in Figiure B1(b),(c), and (d), respectively.

* Corresponding author (email: zhouyi@mail.sitp.ac.cn, jianxinchen@mail.sitp.ac.cn)

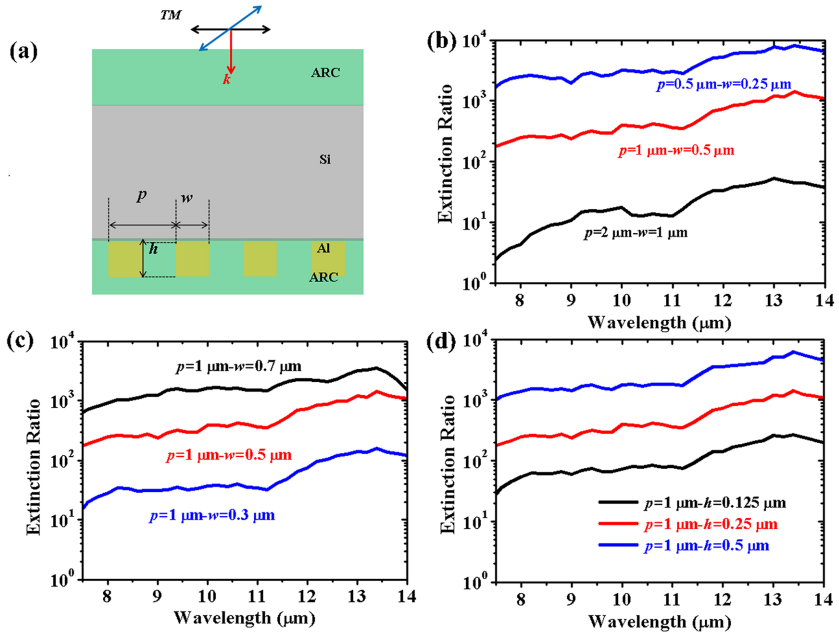

Figure B1 (a) Schematic diagram of the subwavelength metal grating. The ER spectra with different (b) periods, (c) linewidths, and (d) heights.

Appendix C Simulation and theory results of super pixel PI-FPA

To pursue a higher ER PI-FPA with mosaic super pixel structure, we also study the crosstalk between adjacent pixels. The adjacent pixels were covered by two polarization gratings with orthogonal directions, corresponding to the Lines 1 and Lines 2, respectively, as shown in the inset of Figure C1(a). All parameters of grating are consistent with those discussed above. Figure C1(a) shows the simulated ER of Line 1 as a function of distance between polarizer and photosensitive elements. As discussed above, the ER decreases with increasing distance. The ER was also calculated by the ratio between the region 0 to 15 m and 15 to 30 m of the integral electric field intensity using diffraction theory [7–9], which is in good agreement with the results of device simulation. When the distance is more than 40 m. It is found that the ER is less than 10:1 due to the optical crosstalk caused by light diffraction from the adjacent pixel, which can be clearly illustrated from the electric field distribution with the distance is 5, 50, and 200 m, respectively, as shown in Figure C1(b). Our simulation results show that the key to improve the ER is to integrate grating directly on the device surface, which will be studied in our later work.

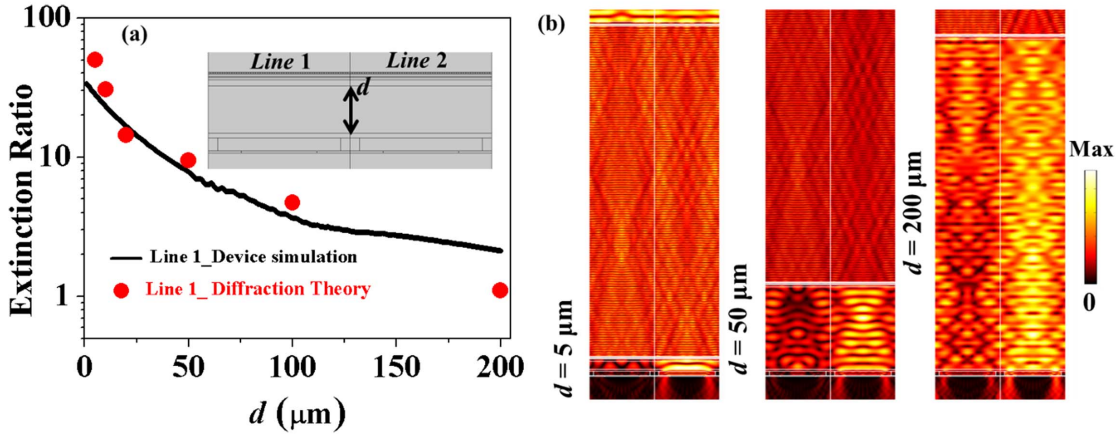

Figure C1 (a) The simulated ER of Line 1 is a function of distance between polarizer and photosensitive elements. The red dot is the ER calculated by diffraction theory. The inset of (a) is the structure of adjacent pixels covered by two polarization gratings with orthogonal directions. (b) The device simulated electrical field distribution with the distance is 5, 50, and 200 m, respectively.

References

1 Jacobs R B, Shanmugam M, Jain N, et al. Extraordinary Photoresponse in Two-Dimensional In2Se3 Nanosheets. ACS Nano, 2014,8:514-21.
2 De Nicola F, Puthiya Purayil N S, Miseikis V, et al. Graphene Plasmonic Fractal Metamaterials for Broadband Photodetectors. Scientific Reports, 2020,10:6882
3 Cirac C, Urzhumov Y, Smith D R. Far-field analysis of axially symmetric three-dimensional directional cloaks. Optics Express, 2013,21:9397-406
4 Wang S, Yoon N, Kamboj A, et al. Ultra-thin enhanced-absorption long-wave infrared detectors. Applied Physics Letters, 2018,112:091104
5 Jin J. The Finite Element Method in Electromagnetics, 3rd Edition. Hoboken, New Jersey: John Wiley & Sons, 2014
6 Chandola A, Pino R, Dutta P S. Below bandgap optical absorption in tellurium-doped GaSb. Semiconductor Science and Technology, 2005,20:886-93
7 Firstenberg O, London P, Shuker M, et al. Reversal and directional bias of optical diffraction. Nature Physics, 20095:665-8
8 Esmer G. Accurate diffraction field calculation method based on L1 -norm minimization from three-dimensional objects. Appl Opt, 2019,58:A267
9 Hu Y, Wang Z, Wang X, et al. Efficient full-path optical calculation of scalar and vector diffraction using the Bluestein method. Light: Science & Applications, 2020,9:119